

Reanalysis of L-band Brightness Predicted by the LSP/R Model for Prairie Grassland: Incorporation of Rough Surface Scattering

Y.-A. Liou, *Member, IEEE*, K.-S. Chen, *Senior Member, IEEE*, and T.-D. Wu

Abstract—L-band brightness predicted by the land surface process/radiobrightness (LSP/R) model for prairie grassland appears to be somewhat lower than expected [1]. A crucial reason for the underestimate of the L-band brightness is that the soil surface was treated as smooth. In this paper, surface scattering of the soil determined by the IEM model is incorporated into the LSP/R model to examine its impact on the predicted L-band brightness. Eight sets of surface parameters, two correlation lengths (L) of 3 and 6 cm \times 4 root mean squared (RMS) heights (σ) of 0.3, 0.6, 0.8, and 1.0 cm, are utilized to characterize the emission of the soil surface. It is found that H-polarized, L-band brightness is expectedly increased by different levels for all of the eight rough surface cases compared to the smooth surface case. The increase in the average of the H-polarized, L-band brightness is by as much as 13.2 K for the case with $L = 3$ cm and $\sigma = 1.0$ cm. In addition, L-band's sensitivity to soil moisture is found to be approximately equal with and without the scattering effects. An increase in H-polarized, L-band brightness by about 12 K at the end of a 14-day simulation by the LSP/R model is in response to a decrease in soil moisture by 7% for all of the nine cases of concern (eight rough plus one smooth soil surfaces).

Index Terms—L-band brightness temperature, polarization index, surface scattering.

I. INTRODUCTION

SURFACE temperature, and water in soil and vegetation that is available to the atmosphere play a key role in the land-air exchanges of energy and moisture so that they become key parameters in atmospheric models for continental weather and climate ([2]–[5]). In addition, they govern infrared and microwave emission of the land surface. This allows one to infer surface temperature [6] and moisture [7], [8], and to estimate surface heat fluxes [9], [10] from satellite imagery, and to assimilate satellite-observed biophysical parameters in land surface process models for climate models [11].

With the needs of satellite data in weather and climate models, the accuracy of forward models to calculate radiometric emission from natural land surfaces is of increasing importance. A series of LSP/R models have been developed to

capture land-air interactions and predict microwave characteristics for bare soils and prairie grassland for the past few years ([1],[12]–[14]). Liou and England [12] developed an annual temperature and radiobrightness model for moist soils whose results demonstrated a significant influence of seasonal history on the surface temperature. This annual model was then refined to take into account coupled heat and moisture transport in unfrozen soils [13], and in freezing soils [14]. Recently, the LSP/R model was further improved to couple heat and moisture transport within prairie grassland [1]. While this prairie LSP/R model was validated with observations from a field campaign, the assumption of a smooth soil surface in its R module is simple and can be improved by taking into account the effect of rough surface scattering. In addition, the LSP/R model seems to underestimate L-band brightness (Schmugge, T. J., 1997, personal communication). Moreover, it was suggested that the requirement for the accuracy in computing bistatic scattering coefficients should be within 1% in order to obtain reliable estimates of rough surface emissivities for passive remote sensing applications [15]. However, it is almost impossible to achieve this requirement, an adoption of a surface scattering model must be carefully determined.

In this paper, the IEM surface scattering model is incorporated into the LSP/R model for prairie grassland to investigate the influence of surface scattering from the soil on the L-band radiometric signatures. L-band has been recognized as an appropriate channel for mapping surface soil moisture ([16]–[19]). Descriptions of the LSP/R model and IEM model, and their validations are given in Section II. Results of numerical simulations are presented in Section III.

II. LSP/R AND IEM MODELS

A. LSP/R Model

The LSP/R model consists of two modules, an LSP module and an R module [1]. The LSP module simulates the exchanges of energy and moisture among air, vegetation, and soil. The R module estimates the brightness of the vegetated-cover terrains by treating the soil surface as smooth. As shown in Fig. 1, the total brightness of the module is comprised of the following four components.

- Tb_s soil brightness attenuated by one trip through the canopy;
- $Tb_{c,d}$ downwelling canopy brightness reflected by the soil and attenuated by one trip through the canopy;

Manuscript received May 11, 1999; revised November 29, 2000. This work was supported by the National Science Council Grant NSC89-2111-M-008-025-AP3.

Y.-A. Liou and K.-S. Chen are with the Center for Space and Remote Sensing Research and the Institute of Space Science National Central University, Chung-Li, Taiwan 320 (e-mail: yueian@csr.ncu.edu.tw).

T.-D. Wu is with the Precision Instrument Development Center National Science Council, Hsinchu, Taiwan 300.

Publisher Item Identifier S 0196-2892(01)00479-X.

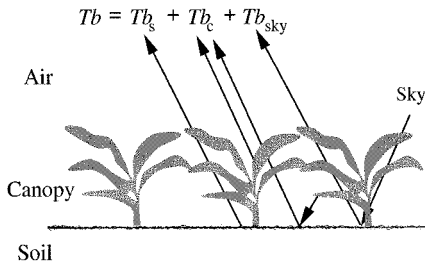


Fig. 1. Radiobrightness components of the R module.

$Tb_{c,u}$ upwelling canopy brightness
 Tb_{sky} sky brightness reflected by the soil and attenuated by two trips through the canopy.

That is

$$\begin{aligned} Tb_s &= T_{s,e}(1 - R_{F,p}(\mu))e^{-\tau_0/\mu} \\ Tb_{c,d} &= T_{c,e}(1 - e^{-\tau_0/\mu})R_{F,p}(\mu)e^{-\tau_0/\mu} \\ Tb_{c,u} &= T_{c,e}(1 - e^{-\tau_0/\mu}) \\ Tb_{sky} &= T_{sky}R_{F,p}(\mu)e^{-2\tau_0/\mu} \end{aligned} \quad (1)$$

where

$T_{s,e}$ effective emitting temperature of the soil [13], [14], [1], K;
 $R_{F,p}$ Fresnel reflectivity of the moist soil for polarization p ;
 μ cosine of the SSM/I incidence angle of 53° ;
 $T_{c,e}$ effective emitting temperature of the canopy, K;
 τ_0 optical depth of the air-grass mixture layer, nepers.

To run the LSP/R model for the purpose of validation, the model was driven by meteorological and sky radiance data from the radiobrightness energy balance experiment (REBEX-1) on prairie grassland near Sioux Falls, SD, during the fall and winter of 1992-1993 [20]. Model predictions were compared with 995 consecutive REBEX-1 observations over a 14-day period in October. The special sensor microwave/imager (SSM/I) channels (19, 22, 37, and 85 GHz), and L-band were chosen in the study so that an incidence angle of 53° was used to compute the radiobrightnesses. While the H-polarized, 19 GHz brightnesses were shown to agree with observations from REBEX-1, the 37 GHz brightnesses were found to be overestimated due to the ignorance of scatter darkening. Moreover, predictions of H-polarized, L-band brightnesses were considered to be lower than expected (Schmugge, 1997, personal communication). A crucial reason for the underestimate of the L-band brightnesses is that surface scattering from the soil was not taken into account. To investigate the impact of soil surface scattering on the L-band radiometric signatures, the IEM model is utilized to determine the surface scattering from the soil that is subsequently incorporated into the LSP/R model in the current presentation.

B. IEM Model

Among the rough surface scattering models, the IEM rough surface scattering model is of a major one [21]. It was first developed to describe electromagnetic wave scattering for a randomly rough, perfectly conducting surface [22], and later, for a randomly rough dielectric surface [23]. The IEM surface scattering

model was then extended to take into account the influence of multiple scattering from two surface points neither near nor far [24], [25], and applied to develop a transition model for the reflection coefficient in surface scattering [26]. The extended IEM surface scattering model was validated with measurements acquired at the University of Texas, Arlington, for a rough perfectly conducting surface, and with those acquired at the European Microwave Signature Laboratory (EMSL), Ispra, Italy, for a very rough dielectric surface.

The emissivity of the soil is expressed as

$$\begin{aligned} e_p(\theta) &= 1 - R_p(\theta) \\ &= 1 - \frac{1}{4\pi \cos \theta} \int_0^{2\pi} \int_0^{\pi/2} \\ &\quad \cdot [\sigma_{pp}^o(\theta, \theta_s; \phi_s - \phi) + \sigma_{qp}^o(\theta, \theta_s; \phi_s - \phi)] \\ &\quad \cdot \sin \theta_s d\theta_s d\phi_s - R_{F,p}(\theta)e^{-(4\pi \cos / \lambda)^2} \end{aligned} \quad (2)$$

where

R_p reflectivity;
 $\sigma_{pp}^o/\sigma_{qp}^o$ like-/cross-polarized bistatic scattering coefficient that is estimated by the IEM model [26];
 θ and ϕ spherical coordinates;
 subscript s represents the direction of the scattered power;
 $e^{-(4\pi \cos / \lambda)^2}$ roughness factor to correct the specular coherent term;
 λ wavelength of the operating frequency.

(2) is appropriate for a half-space lossy medium with negligible power transmitted into the medium.

To validate the emissivity predicted by the IEM model, estimates of the emissivity based on (2) are compared with measurements from a moderately-rough surface reported by the EMSL Joint Research Center, European Commission (EMSL/JRC), Ispra, Italy [27]. The rough surface is a Gaussian correlated surface with an RMS height of 0.4 cm and a correlation length of 6.0 cm. Fig. 2 shows V- and H-polarized emissivities at 6.8 and 10.6 GHz estimated by the IEM model for incidence angles from 20 to 60° at an interval of 5° , and acquired by EMSL/JRC. Model predictions agree with measurements very well. Table I lists the standard deviations in H-polarized (V-polarized) emissivity between model predictions and observations. Good agreements enable us to conduct further numerical simulations by incorporating the IEM model into the prairie LSP/R model, as discussed in Section III. Emissivity measurements are not available for L-band, so we cannot show the similar comparison for L-band.

Note that an exponential correlation function (ECF) is often found to best characterize the measured surfaces of interest [28]. Hence, it is a common practice to describe a naturally rough surface with an ECF as we present in this paper. Nevertheless, the ECF is not differentiable at the origin and cannot be used to define an RMS slope for rough surfaces [21]. We are unaware of measurements from laboratory-controlled experiments for exponential correlated surfaces, so that the use of the IEM theory is validated by comparing its bistatic scattering predictions with measurements from Gaussian correlated surfaces. For the sake of comparison, predictions from the use of the IEM

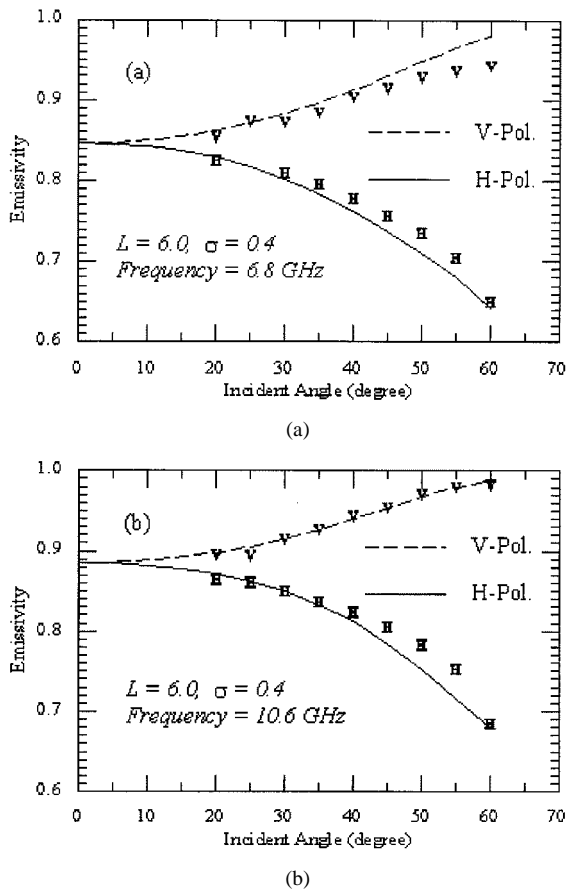


Fig. 2. Angular trends of H- and V-polarized emissivities at 6.8 and 10.6 GHz predicted by the IEM model and acquired by EMSL/JRC.

TABLE I

STANDARD DEVIATIONS (SD) IN H- AND V-POLARIZED EMISSIVITY BETWEEN PREDICTIONS FROM THE IEM MODEL AND THE CORRESPONDING MEASUREMENTS ACQUIRED BY THE EMSL/JRC

Frequency, GHz	L , cm	σ , cm	H-pol SD	V-pol SD
6.8	6.0	0.4	0.0098	0.0122
10.6	6.0	0.4	0.0150	0.0045

theory for Gaussian correlated surfaces are also presented after the treatments of exponential correlated surfaces are detailed in Section III.

III. NUMERICAL SIMULATIONS

A. Exponential Correlated Surfaces

The LSP/R model with incorporation of the IEM model is used to determine the L-band brightnesses for eight exponential correlated surfaces, two correlation lengths of 3 and 6 cm \times 4, and RMS heights of 0.3, 0.6, 0.8, and 1.0 cm. The simulations are executed for the same 14-day period used to validate the LSP/R model so that model predictions of L-band brightness can be compared. The ECF can be written as

$$\rho(\tau) = e^{-(\tau/L)} \tag{3}$$

where L is the correlation length [23].

Fig. 3 shows H-polarized, L-band brightnesses versus daynumber for (a) $L = 3$ cm and (b) $L = 6$ cm, and versus

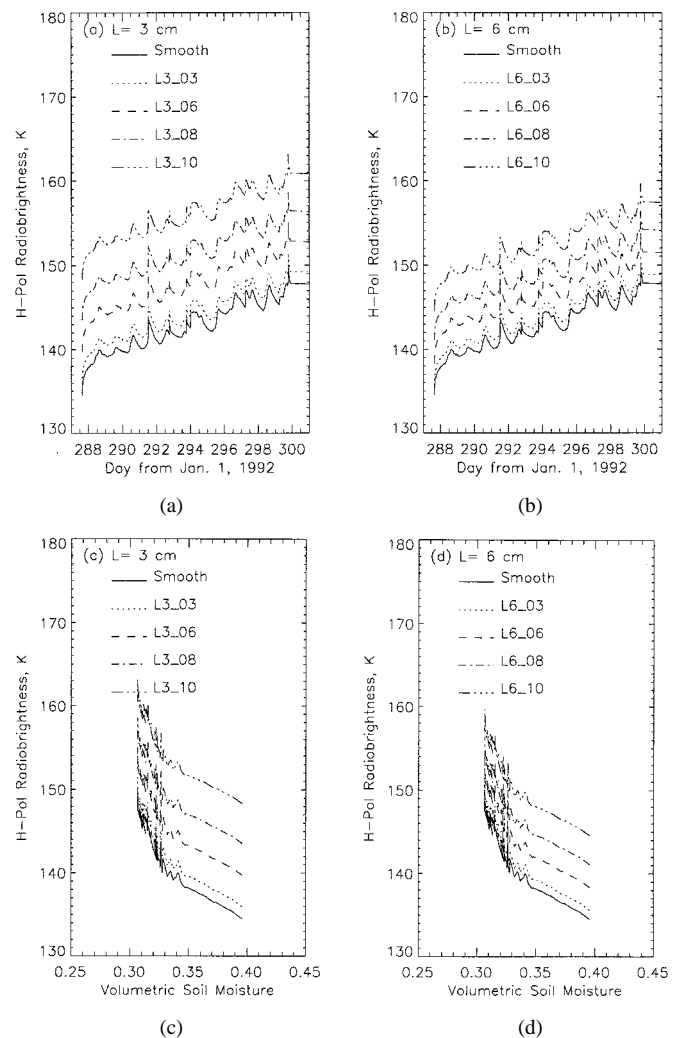


Fig. 3. H-polarized, L-band brightnesses versus daynumber for (a) $L = 3$ cm and (b) $L = 6$ cm, and versus soil moisture for (c) $L = 3$ cm and (d) $L = 6$ cm. The corresponding results for the smooth soil surface case are also included. Notations used in the figure are explained in Table II.

soil moisture for (c) $L = 3$ cm and (d) $L = 6$ cm. The corresponding results for the smooth soil surface case are also plotted in the figure. Notations used in the figure stand for the smooth surface case and eight kinds of rough surfaces as explained in Table II. It is observable that the predicted L-band brightnesses appear to increase with daynumber at the same rate during the 14-day period for all of the nine surfaces, one smooth and eight rough surfaces. The increases in L-band brightness are about 12 K for all of the nine cases. They are primarily in response to a decrease in soil moisture of about 7%. This indicates that the sensitivity of L-band brightness to soil moisture is about equal for the nine cases. In addition, we observe that L-band brightnesses are higher for all of the rough surface cases than the smooth surface case. The increases in the average of H-polarized, L-band brightnesses range from 1.1 K for $L = 6$ cm and $\sigma = 0.3$ cm to 13.2 K for $L = 3$ cm and $\sigma = 1.0$ cm, as shown in Table II.

In contrast, V-polarized, L-band brightnesses are decreased by different amounts for the eight rough surface cases compared to the smooth soil surface case. Fig. 4 shows the V-polarized, L-band brightnesses versus daynumber for (a) $L = 3$ cm and

TABLE II
NOTATIONS USED TO REPRESENT THE EIGHT ROUGH SURFACE CASES, AND INCREASES IN THE AVERAGE OF H-POLARIZED, L-BAND BRIGHTNESSES (ΔTb_H) AND DECREASES IN V-POLARIZED, L-BAND BRIGHTNESSES (ΔTb_V) FOR EIGHT ROUGH SURFACE CASES COMPARED TO THE SMOOTH SOIL SURFACE CASE

Cases	L , cm	σ , cm	ΔTb_H , K	ΔTb_V , K
L3_03	3.0	0.3	1.39	-0.39
L3_06	3.0	0.6	4.99	-0.94
L3_08	3.0	0.8	8.63	-1.46
L3_10	3.0	1.0	13.20	-2.05
L6_03	6.0	0.3	1.06	-0.52
L6_06	6.0	0.6	3.68	-1.47
L6_08	6.0	0.8	6.34	-2.39
L6_10	6.0	1.0	9.68	-3.50

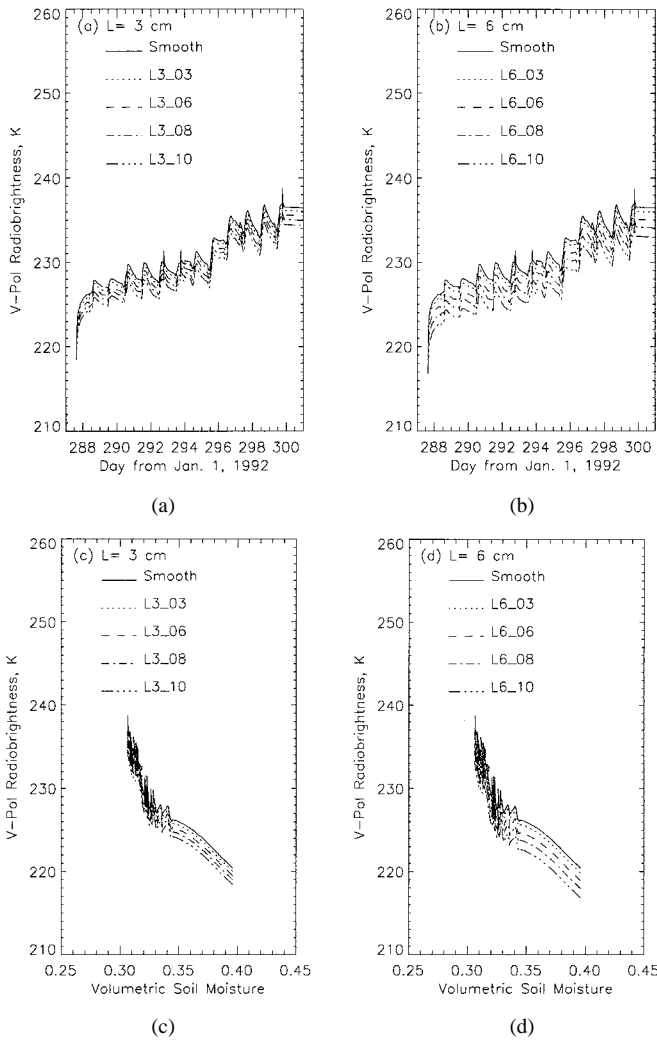


Fig. 4. V-polarized, L-band brightnesses versus daynumber for (a) $L = 3$ cm and (b) $L = 6$ cm, and versus soil moisture for (c) $L = 3$ cm and (d) $L = 6$ cm. The corresponding results for the smooth soil surface case are also included.

(b) $L = 6$ cm, and versus soil moisture for (c) $L = 3$ cm and (d) $L = 6$ cm. The decreases in V-polarized, L-band brightness are listed in Table II. We notice that the magnitudes of ΔTb_V appear to be relatively small compared to those of ΔTb_H . The largest decrease occurs by -3.5 K for the case with $L = 6$ cm and $\sigma = 1.0$ cm. This indicates that the smooth surface high emissivity is due to the Brewster angle effect and is partially reduced by surface roughness. Scattering results in depolarization of the

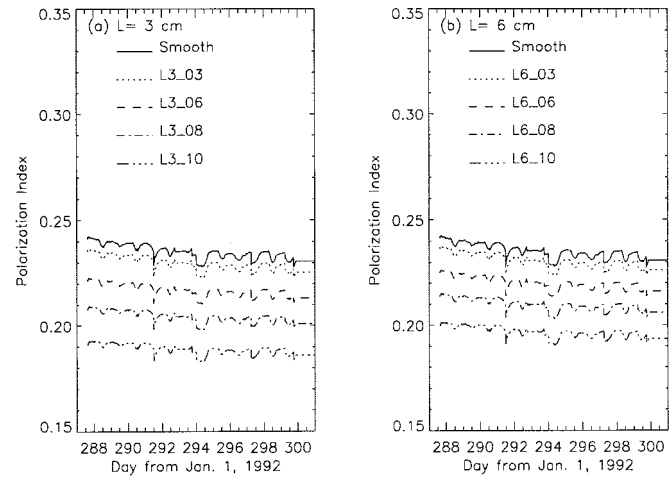


Fig. 5. L-band polarization index based on the 14-day simulations of the prairie LSP/R model with and without incorporation of the IEM model.

surface emission so that L-band brightnesses are increased for the H-polarization but decreased for the V-polarization. That is, the difference in V- and H-polarized, L-band brightnesses is decreased with increasing surface roughness.

An alternative way to quantify the depolarization of the surface emission caused by the roughness is through an evaluation of the polarization index (PI) defined as

$$PI = \frac{Tb_V - Tb_H}{Tb_V + Tb_H} \quad (4)$$

where Tb_V is the V-polarized brightness, and Tb_H is the H-polarized brightness. Fig. 5 shows the L-band polarization index based on the 14-day simulations of the prairie LSP/R model with and without incorporation of the IEM rough surface scattering model. Similarly, PI is decreased with increasing surface scattering.

B. Gaussian Correlated Surfaces

To examine the impact of correlation function on L-band brightness, the LSP/R model and the IEM model are simulated for eight Gaussian correlated surfaces. The conditions of roughness for the eight Gaussian correlated surfaces are as same as those used for the exponential correlated surfaces. Fig. 6 shows the V-polarized, L-band brightnesses versus daynumber for (a) $L = 3$ cm and (b) $L = 6$ cm, and versus soil moisture for (c) $L = 3$ cm and (d) $L = 6$ cm for the Gaussian correlated surfaces. The changes in both H-polarized and V-polarized, L-band brightness are listed in Table III. H-polarized, L-band brightnesses are not shown because they are less influenced by the correlation function than the V-polarized, L-band brightnesses. A comparison between Figs. 4 and 6 and a comparison between Tables II and III demonstrate that the use of both correlation functions results in similar impacts on L-band brightness. As examples, the sensitivity of L-band brightness to soil moisture is about equal for all rough surfaces, and it is little correlation function-dependent, and the magnitudes of ΔTb_H and ΔTb_V increase with increasing RMS height for the same correlation length. The exception is that the decrease in Tb_V is more profound for Gaussian correlated surfaces than exponential correlated surfaces. This suggests that the IEM

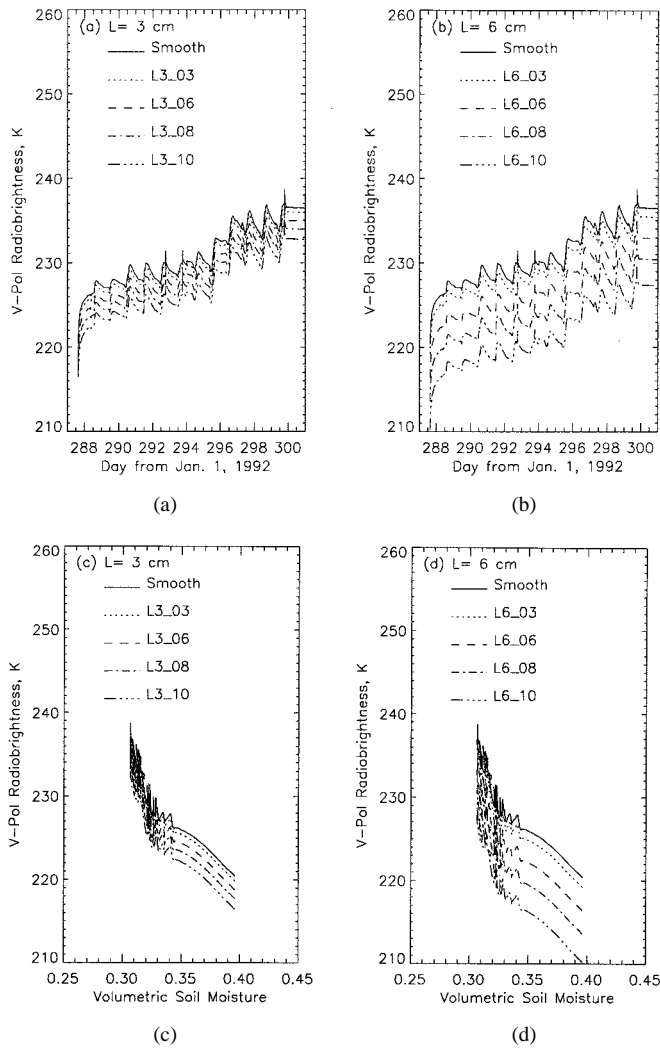


Fig. 6. V-polarized, L-band brightnesses versus daynumber for (a) $L = 3$ cm and (b) $L = 6$ cm, and versus soil moisture for (c) $L = 3$ cm and (d) $L = 6$ cm for the eight Gaussian correlated surfaces.

TABLE III

INCREASES IN THE AVERAGE OF H-POLARIZED, L-BAND BRIGHTNESSES (ΔTb_H) AND DECREASES IN V-POLARIZED, L-BAND BRIGHTNESSES (ΔTb_V) FOR THE EIGHT GAUSSIAN CORRELATED SURFACES COMPARED TO THE SMOOTH SOIL SURFACE CASE

Cases	L , cm	σ , cm	ΔTb_H , K	ΔTb_V , K
L3_03	3.0	0.3	1.44	-0.55
L3_06	3.0	0.6	5.18	-1.56
L3_08	3.0	0.8	8.94	-2.55
L3_10	3.0	1.0	13.60	-3.75
L6_03	6.0	0.3	0.91	-1.08
L6_06	6.0	0.6	3.08	-3.66
L6_08	6.0	0.8	5.28	-6.22
L6_10	6.0	1.0	8.04	-9.34

model predicts stronger bistatic scattering for the Gaussian correlated surfaces than the exponential correlated surfaces for V-polarization at L-band for the incident angle of our concern since the specular coherent term in (2) is correlation function independent. Consequently, depolarization of the surface emission at L-band is more profound for the Gaussian

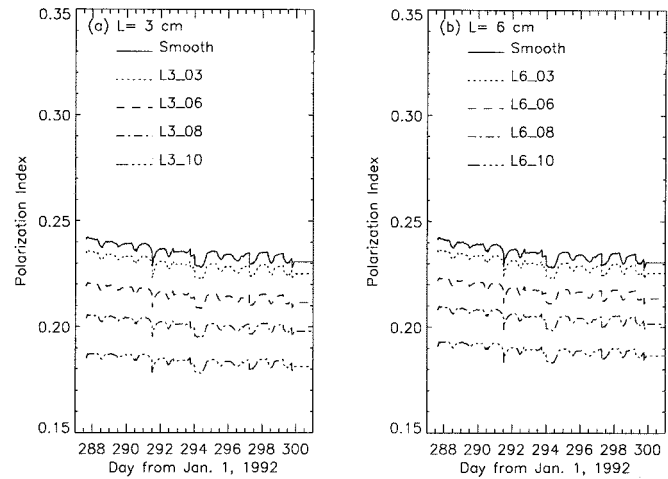


Fig. 7. L-band polarization index based on the 14-day simulations of the prairie LSP/R model with and without incorporation of the IEM model for the eight Gaussian correlated surfaces.

correlated surface as shown in Fig. 7. It is clearly observable that PI values are decreased most obvious for the case with $L = 6$ cm and $\sigma = 1.0$ cm than the other cases.

IV. CONCLUSIONS

L-band radiometric signatures are re-analyzed using predictions from the LSP/R model with and without incorporation of the rough surface scattering. The scattering from soil surface is estimated by the IEM model. While there are no field experiments to verify the L-band emissivities predicted by the IEM model, we do validate the model predictions of emissivities at 6.8 and 10.6 GHz. Good agreements in emissivity at the two frequencies between model predictions and measurements acquired by the EMSL/JRC are achieved for two moderately rough surfaces.

Upon validating the emissivity predictions from the IEM model, the model is incorporated into the LSP/R model to calculate surface scattering from the soil at L-band. Eight sets of surface parameters are considered. Very encouraging results are obtained because H-polarized, L-band brightnesses are increased by different amounts for all of the eight rough surface cases compared to the smooth soil surface case, whose predictions were considered to be somewhat lower than expected (Schmugge, T. J., 1997, personal communication). The increases in the average of the H-polarized, L-band brightness range from 1.1 K for $L = 6$ cm and $\sigma = 0.3$ cm to 13.2 K for $L = 3$ cm and $\sigma = 1.0$ cm. In contrast, V-polarized, L-band brightnesses are decreased since surface scattering results in depolarization of the soil surface emission. The decreases in the average of the V-polarized, L-band brightness range from 0.39 K for $L = 3$ cm and $\sigma = 0.3$ cm to -3.50 K for $L = 6$ cm and $\sigma = 1.0$ cm.

In addition, L-band's sensitivity to soil moisture is shown to remain about the same with and without the scattering effects. An increase in H-polarized, L-band brightness by about 12 K at the end of the 14-day simulations is in response to a decrease in soil moisture by 7% for the nine cases of interest. There is almost no difference in L-band's sensitivity to soil moisture, probably because the factors dominating surface scattering are not changed during the 14-day period of the simulations.

ACKNOWLEDGMENT

The authors would like to thank the anonymous referees for their suggestions for improving the manuscript.

REFERENCES

- [1] Y.-A. Liou, J. Galantowicz, and A. W. England, "A land surface process/radiobrightness model with coupled heat and moisture transport for prairie grassland," *IEEE Trans. Geosci. Remote Sensing*, vol. 37, pp. 1848–1859, July 1999.
- [2] P. R. Rowntree and J. R. Bolton, "Simulation of the atmospheric response to soil moisture anomalies over Europe," *Q. J. R. Meteorol. Soc.*, vol. 109, pp. 501–526, 1983.
- [3] W. M. Cunnington and P. R. Rowntree, "Simulation of the Saharan atmosphere-dependence on moisture and albedo," *Q. J. R. Meteorol. Soc.*, vol. 112, pp. 971–999, 1986.
- [4] J.-F. Mahfouf, E. Richard, and P. Mascart, "The influence of soil and vegetation on the development of mesoscale circulations," *J. Appl. Meteorol.*, vol. 26, pp. 1483–1495, 1987.
- [5] D. P. Rowell and C. Blondin, "The influence of soil wetness distribution on short-range rainfall forecasting in the West African Sahel," *Q. J. R. Meteorol. Soc.*, vol. 116, pp. 1471–1485, 1990.
- [6] M. Sugita and W. Brutsaert, "Comparison of land surface temperatures derived from satellite observations with ground truth during FIFE," *Int. J. Remote Sensing*, vol. 14, pp. 1659–1676, 1993.
- [7] B. J. Choudhury and R. E. Golus, "Estimating soil wetness using satellite data," *Int. J. Remote Sensing*, vol. 9, pp. 1251–1257, 1988.
- [8] N. U. Ahmed, "Estimating soil moisture from 6.6 GHz dual polarization, and/or satellite derived vegetation index," *Int. J. Remote Sensing*, vol. 16, pp. 687–708, 1995.
- [9] W. Brutsaert and M. Sugita, "Regional surface fluxes from satellite-derived surface temperatures (AVHRR) and radiosonde profiles," *Bound.-Layer Meteorol.*, vol. 58, pp. 355–366, 1992.
- [10] X. Huang, T. J. Lyons, R. C. G. Smith, J. M. Hacker, and P. Schwerdtfeger, "Estimation of surface energy balance from radiant surface temperature and NOAA AVHRR sensor reflectances over agricultural and native vegetation," *J. Appl. Meteorol.*, vol. 32, pp. 1441–1449, 1993.
- [11] P. J. Sellers, S. O. Los, C. J. Tucker, C. O. Justice, D. A. Dazlich, G. J. Collatz, and D. A. Randall, "A revised land surface parameterization (SiB2) for atmospheric GCM's. Part II: The generation of global fields of terrestrial biophysical parameters from satellite data," *J. Climate*, vol. 9, pp. 706–737, 1996.
- [12] Y.-A. Liou and A. W. England, "Annual temperature and radiobrightness signatures for bare soils," *IEEE Trans. Geosci. Remote Sensing*, vol. 34, pp. 981–990, 1996.
- [13] —, "A land surface process/radiobrightness model with coupled heat and moisture transport in soil," *IEEE Trans. Geosci. Remote Sensing*, vol. 36, pp. 273–286, 1998.
- [14] —, "A land surface process/radiobrightness model with coupled heat and moisture transport for freezing soils," *IEEE Trans. Geosci. Remote Sensing*, vol. 36, pp. 669–677, 1998.
- [15] Q. Li, L. Tsang, K. Pak, and C.-H. Chan, "Scattering of electromagnetic waves and emissivities of random rough dielectric lossy surfaces with the physics-based two grid method combined with the sparse-matrix canonical grid method," in *PIERS'99*, Taipei, China, Mar. 22–26, 1999.
- [16] J. R. Wang, J. C. Shiue, T. J. Schmugge, and E. T. Engman, "Mapping surface soil moisture with L-band radiometric measurements," *Remote Sens. Environ.*, vol. 27, pp. 305–312, 1989.
- [17] J.-P. Wigneron, Y. Kerr, A. Chanzy, and Y.-Q. Jin, "Inversion of surface parameters from passive microwave measurements over a soybean field," *Remote Sens. Environ.*, vol. 46, pp. 61–72, 1993.
- [18] Y. A. Liou, Y. C. Tzeng, and K. S. Chen, "The use of neural networks in radiometric studies of land surface parameters," *Proc. NSC Part A: Phys. Sci. Eng.*, vol. 23, no. 4, pp. 511–518, 1999.
- [19] —, "A neural network approach to radiometric sensing of land surface parameters," *IEEE Trans. Geosci. Remote Sensing*, vol. 37, pp. 2718–2724, Nov. 1999.
- [20] J. F. Galantowicz and W. England, Principal Investigator, "Field data report for the First Radiobrightness Energy Balance Experiment (REBEX-1)," Radiation Lab., Univ. Michigan, Ann Arbor, Tech. Rep. RL-913, Feb. 1995.
- [21] A. F. Fung, *Microwave Scattering and Emission Models and Their Applications*. Norwell, MA: Artech House, 1994.
- [22] A. F. Fung and G. W. Pan, "A scattering model for perfectly conducting random surface: I. Model development. II. Range of validity," *Int. J. Remote Sensing*, vol. 8, pp. 1579–1605, 1987.
- [23] A. F. Fung, Z. Li, and K. S. Chen, "Backscattering from a randomly rough dielectric surface," *IEEE Trans. Geosci. Remote Sensing*, vol. 30, pp. 356–369, 1992.
- [24] C. Y. Hsieh, A. F. Fung, G. Nesti, A. J. Sieber, and P. Coppo, "A further study of the IEM surface scattering model," *IEEE Trans. Geosci. Remote Sensing*, vol. 35, pp. 901–909, 1997.
- [25] K. S. Chen, T. D. Wu, M. K. Tsay, and A. K. Fung, "A note on the multiply scattering in IEM model," *IEEE Trans. Geosci. Remote Sensing*, vol. 38, pp. 249–256, Jan. 2000.
- [26] —, "A transition model for the reflection coefficient in surface scattering," in *Proc. Int. Geosci. Remote Sensing Symp.*, Seattle, WA, 1998, pp. 2375–2377.
- [27] P. Coppo, S. Lolli, G. Macelloni, G. Nesti, P. Pampaloni, R. Ruisi, and D. Tarchi, "Experimental validation of surface scattering and emission models," in *Proc. IGARSS'97*, Singapore, Aug. 3–8, 1997.
- [28] J. A. Ogilvy, *Theory of Wave Scattering from Random Rough Surfaces*. Philadelphia, PA: IOP, 1992, p. 14.

Y. A. Liou (S'91–M'96) received the B.S. degree in electrical engineering from National Sun Yat-Sen University, Kaohsiung, Taiwan, R.O.C., in 1987, and the M.S.E. degree in electrical engineering, the M.S. degree in atmospheric and space sciences, and Ph.D. degree in electrical engineering and atmospheric, oceanic, and space sciences from the University of Michigan, Ann Arbor, in 1992, 1994, and 1996, respectively.

From 1989 to 1990, he was a Research Assistant with the Robotics Laboratory, National Taiwan University, Taipei. From 1991 to 1996, he was a Graduate Research Assistant with the Radiation Laboratory, University of Michigan, Ann Arbor, where he developed land-air interaction and microwave emission models for prairie grassland. In 1996, he joined the Faculty of the Center for Space and Remote Sensing Research and the Institute of Space Science, National Central University, Chung-Li, Taiwan, where he is now an Associate Professor. His current research activities include GPS meteorology and ionosphere, remote sensing of the atmosphere and land surface, application of neural networks and fuzzy systems in inversion problems, and satellite communications. He is a Principal Investigator on projects sponsored by the National Science Council of Taiwan (NSC) and the ONR. He has published more than 20 referred journal papers and more than 50 international conference papers. He is a referee for *Terrestrial, Atmospheric and Oceanic Sciences and Water Resources Research, Earth, Planets, and Space*.

Dr. Liou is listed in *Who's Who in the World*. He is a referee for IEEE TRANSACTIONS ON GEOSCIENCE AND REMOTE SENSING and was a recipient of Research Awards from NSC in 1999 and 2000. He served as a Technical Committee member of PIERS 1999 held in Taipei. He is a member of the American Geophysical Union and the American Meteorological Society.

K. S. Chen (S'86–M'90–SM'98) received the B.S.E.E. from National Taiwan Institute of Technology, Taipei, Taiwan, R.O.C., in 1985, and the M. S. and Ph.D. degrees from the University of Texas, Arlington, in 1987 and 1990, respectively, all in electrical engineering.

From 1985 to 1990, he was with the Wave Scattering Research Center, University of Texas, Arlington. In 1992, he joined the Faculty of the Center for Space and Remote Sensing Research and the Institute of Space Science, National Central University, Chung-Li, Taiwan, as Associate Professor and has been a full Professor since 1996. His research activities involve the areas of microwave remote sensing, image processing, and analysis for satellite and aircraft remote sensing data, radio and microwave propagation, and scattering from terrain and ocean with applications to remote sensing and communications. He has published more than 40 referred journal papers and over 80 international conference papers. He is on the editorial board of the *Journal of Electromagnetic Waves and Applications, Transactions of the Aeronautical and Astronautical Society of the Republic of China*, and *Journal of Chinese Photogrammetry and Remote Sensing*.

Dr. Chen was the recipient of the 1993 Young Scientist Award from the International Union of Radio Science (URSI) and has received numerous research awards from the National Science Council of Taiwan since 1993. He is an Associate Editor of the IEEE TRANSACTIONS ON GEOSCIENCE AND REMOTE SENSING. He served as Technical Chairman of PIERS 1999 held in Taipei, Taiwan.

Tzong-Dar Wu received the B.S., M.S., and Ph.D degrees in electrical engineering from National Central University, Chung-Li, Taiwan, R.O.C., in 1991, 1993, and 1999, respectively.

From 1997 to 1998, he was a Visiting Scholar with the Wave Scattering Research Center, Department of Electrical Engineering, University of Texas, Arlington. He is currently working as an Associate Researcher with the Precision Instrument Development Center, National Science Council, Taiwan. His research interests have been in the areas of wireless communication with emphasis on channel modeling, simulation, and measurements. Recently, he has been working on terrain propagation and scattering with applications to microwave remote sensing and radio communication.